The Journal of Molecular Diagnostics, Vol. 24, No. 6, June 2022

ELSEVIER

the Journal of Molecular Diagnostics
jmdjournal.org

Unraveling Structural Rearrangements of the *CFH* Gene Cluster in Atypical Hemolytic Uremic Syndrome Patients Using Molecular Combing and Long-Fragment Targeted Sequencing

Nikolai Tschernoster,[*†‡] Florian Erger,[†‡] Patrick R. Walsh,[§] Bairbre McNicholas,[¶] Margareta Fistrek,[‖] Sandra Habbig,[**] Anna-Lena Schumacher,[††] Kat Folz-Donahue,[††] Christian Kukat,[††] Mohammad R. Toliat,[*] Christian Becker,[*] Holger Thiele,[*] David Kavanagh,[§] Peter Nürnberg,[*†] Bodo B. Beck,[†‡] and Janine Altmüller[*†‡‡§§]

From the Cologne Center for Genomics,[*] the Center for Molecular Medicine Cologne,[†] the Institute of Human Genetics,[‡] and the Department of Pediatrics,[**] University of Cologne, Faculty of Medicine and University Hospital Cologne, Cologne, Germany; the National Renal Complement Therapeutics Centre,[§] Royal Victoria Infirmary and Translational and Clinical Research Institute, Newcastle University, Newcastle upon Tyne, United Kingdom; the School of Medicine,[¶] National University of Ireland Galway, Galway, Ireland; the Division of Nephrology, Arterial Hypertension Dialysis and Transplantation,[‖] Department of Internal Medicine, University Hospital Center Zagreb, School of Medicine, University of Zagreb, Zagreb, Croatia; the FACS & Imaging Core Facility,[††] Max Planck Institute for Biology of Ageing, Cologne, Germany; the Berlin Institute of Health at Charité—Universitätsmedizin Berlin,[‡‡] Core Facility Genomics, Berlin, Germany; and the Max Delbrück Center for Molecular Medicine in the Helmholtz Association,[§§] Berlin, Germany

Accepted for publication February 25, 2022.

Address correspondence to Janine Altmüller, M.D., Max Delbrück Center for Molecular Medicine in the Helmholtz Association, Hannoversche Strasse 28, 10115 Berlin, Germany; or Nikolai Tschernoster, M.Sc., Cologne Center for Genomics, University of Cologne, Faculty of Medicine and University Hospital Cologne, Weyertal 115b, 50931 Cologne, Germany.
E-mail: janine.altmueller@bih-charite.de or nikolai.tschernoster@uk-koeln.de.

Complement factor H (CFH) and its related proteins have an essential role in regulating the alternative pathway of the complement system. Mutations and structural variants (SVs) of the *CFH* gene cluster, consisting of *CFH* and its five related genes (*CFHR1-5*), have been reported in renal pathologies as well as in complex immune diseases like age-related macular degeneration and systemic lupus erythematosus. SV analysis of this cluster is challenging because of its high degree of sequence homology. Following first-line next-generation sequencing gene panel sequencing, we applied Genomic Vision's Molecular Combing Technology to detect and visualize SVs within the *CFH* gene cluster and resolve its structural haplotypes completely. This approach was tested in three patients with atypical hemolytic uremic syndrome and known SVs and 18 patients with atypical hemolytic uremic syndrome or complement factor 3 glomerulopathy with unknown *CFH* gene cluster haplotypes. Three SVs, a *CFH/CFHR1* hybrid gene in two patients and a rare heterozygous *CFHR4/CFHR1* deletion in *trans* with the common *CFHR3/CFHR1* deletion in a third patient, were newly identified. For the latter, the breakpoints were determined using a targeted enrichment approach for long DNA fragments (Samplix Xdrop) in combination with Oxford Nanopore sequencing. Molecular combing in addition to next-generation sequencing was able to improve the molecular genetic yield in this pilot study. This (cost-)effective approach warrants validation in larger cohorts with CFH/CFHR-associated disease. *(J Mol Diagn 2022, 24: 619—631; https://doi.org/10.1016/j.jmoldx.2022.02.006)*

Complement factor H (CFH) is long known for its essential role in regulation of the alternative pathway of the complement system. The CFH protein family includes the complement regulator CFH and CFH-like protein 1, a shorter alternative splicing product of CFH, as well as the five CFH-related proteins, CFHR1, CFHR2, CFHR3, CFHR4, and CFHR5.[1,2] Together, they form the *CFH* gene

Supported by the Deutsche Forschungsgemeinschaft (DFG; German Research Foundation) clinical research unit (KFO 329) AL901/2-1 and AL901/3-1 (J.A.) and clinical research unit (KFO 329) BE6072/2-1 and BE6072/3-1 (B.B.B.). This work received additional support by the DFG Research Infrastructure as part of the Next Generation Sequencing Competence Network (project 423957469).
B.B.B. and J.A. contributed equally to this work.
Disclosures: None declared.

https://doi.org/10.1016/j.jmoldx.2022.02.006

cluster spanning over approximately 360 kb.[3] Because of successive large genomic duplication events during human evolution, *CFH* and its five related genes (*CFHR1* to *CFHR5*) show high sequence and structural homologies and lie in a head-to-tail arrangement within the regulators of the complement activation gene cluster on chromosome 1q32.[4–6] These genomic structural variants are most probably caused by nonallelic homologous recombination[7,8] and interlocus gene conversion[2] or a mechanism called microhomology-mediated end joining, reported by Challis et al[9] and Francis et al,[10] respectively. The circulating plasma protein CFH is primarily produced in the liver and is composed of individual folding domains called short consensus repeats. CFH's C-terminal region has a surface recognition function, whereas the N-terminal region mediates cofactor and decay-acceleration activity.[11] Zipfel et al[12] reviewed the composition and functionality of CFH and its related proteins in more detail. Mutations and structural variants (SVs) have been reported for atypical hemolytic uremic syndrome (aHUS), glomerulonephritis, immune complex membranoproliferative glomerulonephritis and complement factor 3 glomerulopathy (C3G),[13,14] dense-deposit disease,[15] and systemic lupus erythematosus (SLE).[16] A missense variant in *CFH* (Y402H) has been proposed to be a major risk variant in age-related macular degeneration pathology.[17] In contrast, the common *CFHR3/CFHR1* deletion has been confirmed to protect against age-related macular degeneration as *CFHR3/CFHR1* deletion is less frequent in individuals with age-related macular degeneration pathology than in controls.[18–20] In aHUS, the *CFHR3/CFHR1* deletion is associated as risk factor for the development of anti-CFH autoantibodies, resulting in a disease called deficiency of CFHR plasma proteins and autoantibody-positive form of hemolytic uremic syndrome (DEAP-HUS).[21,22] In addition, the *CFHR3/CFHR1* deletion is proposed to lower the risk of IgA nephropathy.[23] There were also conflicting results published regarding CFH (eg, the possible role of variant Y402H for susceptibility and severity of schizophrenia).[24,25] Noteworthy, just recently, Tang et al[26] showed that there is evidence of increased CFH protein levels in patients with anhedonia in drug-naïve major depression disorder, expanding the spectrum of CFH involvement in a great variety of pathologies.

Atypical Hemolytic Uremic Syndrome

Hemolytic uremic syndrome (HUS; Online Mendelian Inheritance in Man number 235400) is a rare but severe and genetically heterogeneous disease that belongs to the group of thrombotic microangiopathies and arises from an initial endothelial cell injury.[27] aHUS is mainly caused by deregulation of the alternative pathway of the complement system and follows an acute episodic clinical course.[28] The immunohistologic finding of glomerular C3 deposition is termed C3 glomerulopathy (C3G) and represents a separate disease entity. Thrombotic microangiopathy is not observed, and the disease course is often chronic-progressive. However, the pathomechanistic cause of C3G also lies in an inadequately increased activity of the alternative pathway of the complement system.[29] Research into the genetic basis of both aHUS and C3G has identified pathogenic variants, including structural variants in several different complement-associated genes. Genomic aberrations or structural variants affecting the complement factor H (*CFH*) gene cluster were reported in approximately 4.5% of patients, in a cohort of 154 individuals with aHUS analyzed by multiplex ligation-dependent probe amplification (MLPA),[7] and are often caused by nonallelic homologous recombination events.[7,9,10] Incomplete penetrance is frequently observed in families with autosomal dominant aHUS, where unaffected family members carry the causative aberration as well.[30,31] These variants either decrease the activity of the complement-regulating proteins or increase the activity of complement activator proteins, leading to a decreased threshold for inappropriate pathologic complement activation.

The current routine molecular diagnostics for aHUS patients consist of next-generation sequencing (NGS) or Sanger sequencing, augmented by deletion and duplication testing using MLPA.[7,9,32]

CFH/CFHR hybrid gene identification can be performed using either chromosomal microarray[7,33] or PCR-based approaches, the latter of which may also allow for breakpoint detection.[7,9,33] CFH autoantibodies are associated with the frequent homozygous *CFHR3/CFHR1* deletions and are often tested with enzyme-linked immunosorbent assay.[33,34] In a research setting, Cantsilieris et al[4] performed high-quality sequencing, including six primate lineages and multiple human haplotypes, to analyze the evolutionary development of the highly homologous *CFH* gene cluster using bacterial artificial chromosomes, fosmids, and long-read sequencing approaches. The synthesis of hybrid transcripts and secretion of hybrid proteins can be analyzed by Western blot analysis.[7,9]

This study aimed to increase the molecular genetic diagnostic yield of patients presenting with unresolved aHUS and C3G disease by combining NGS with molecular combing and breakpoint identification in the *CFH* gene cluster.

Materials and Methods

Patient Cohort

A total of 21 patients with a clinical diagnosis of aHUS ($n = 15$) or C3G ($n = 6$) were included in this study (Supplemental Table S1). Infection- and medication-associated causes of hemolytic uremic syndrome were excluded in all patients. Three patients with a known structural aberration (F15, F19, and F20) in the *CFH* gene cluster were used as positive controls. DNA of the remaining 18 unresolved patients (the discovery cohort), including two sisters from family 10 with homozygous *CFH*

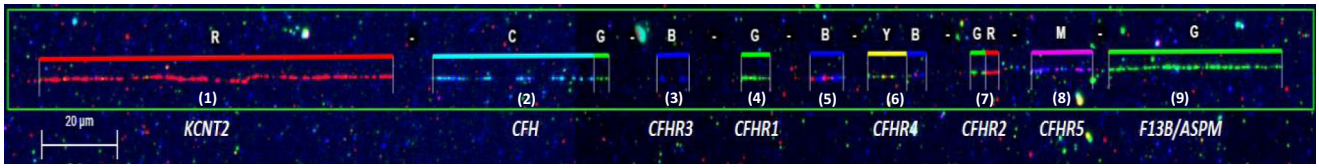

Figure 1 Reference complement factor H (*CFH*) gene cluster on chromosome 1q32. *CFH/CFHR1-5* gene-cluster identification on a hybridized Combicoverslip of a patient with no structural aberrations detected using the FiberStudio software version 2.0.2. All molecular combing images were taken at FiberStudio's zoom level (−7) with a ×40 magnification. Validated signal with labeled genes from left ro right: red, *KCNT2* (1); cyan/green, *CFH* (2); blue, *CFHR3* (3); green, *CFHR1* (4); blue, intronic region (5); yellow/blue, *CFHR4* (6); green/red, *CFHR2* (7); magenta, *CFHR5* (8); green, *F13B* + *ASPM* (9). *CFH* is labeled in cyan with a short region at the C-terminus labeled in green. *CFHR3* labeled in blue, followed by *CFHR1* labeled in green. An intronic region between *CFHR1* and *CFHR4* is labeled in alternating red and blue with a remarkable cyan end. *CFHR4* is labeled in yellow with a short C-terminal region labeled in blue. *CFHR2* is equally labeled in green (N-terminus) and red (C-terminus). *CFHR5* is labeled in magenta. Flanking the *CFH/CFHR* gene cluster, the control gene *KCNT2* (5′) is labeled in red and control gene *F13B* + *ASPM* (3′) is labeled in green. In 10 of the 21 patients, the wild-type *CFH/CFHR* gene cluster appears in its head-to-tail arrangement, as previously described by Heinen et al.[2] Scale bar = 20 µm.

mutations and discordant clinical course,[35] were analyzed at the Institute of Human Genetics of the University Hospital of Cologne for complement-associated nephropathies. Inclusion criteria were a clinical diagnosis of aHUS/renal thrombotic microangiopathy/C3G, no causative variant in the genes associated with aHUS using NGS panel analysis (except F10, this family was screened for the presence of genetic disease modifiers), and availability of a high-molecular-weight DNA sample.

This study was approved by the ethics committee of the Medical Faculty of the University of Cologne (identifier 15-215). All patients gave written informed consent for their participation in this study.

Molecular Combing

Venous blood samples were obtained from each patient for high-molecular-weight DNA isolation and extraction. High-molecular-weight DNA was extracted using the Genomic Vision DNA extraction kit (EXTR-001; Genomic Vision, Bagneux, France), according to the manufacturer's specifications. In short, leukocytes were isolated and embedded into agarose gel plugs. The agarose plugs were treated with proteinase K overnight at 50°C, melted at 68°C, and digested with β agarase at 42°C overnight. High-molecular-weight DNA was released into DNA reservoirs (RES-001) containing 1.2 µL Combing buffer (included in DNA extraction kit; Genomic Vision). Engraved vinyl-silane coated coverslips (COV-002-RUO; Genomic Vision) were embedded into the high-molecular-weight DNA solution. DNA was stretched onto coverslips by pulling the coverslip out of the DNA solution with a constant speed of 300 µm/second using the Fibercomb system (MCS-001; Genomic Vision) and permanently immobilized at 60°C for at least 2 hours. FiberProbes (FB-OD) DNA fluorescent *in situ* hybridization probes were custom designed in cooperation with Genomic Vision. Combed DNA fibers were hybridized with the FiberProbes CFH using a hybridizer (Dako/Agilent, Santa Clara, CA) and corresponding antibodies. Hybridized coverslips were scanned using the FiberVision automated scanner, and the image analysis and signal measurement were done using the FiberStudio software version 2.0.2 (Genomic Vision). Each *CFH* gene cluster signal was manually marked, and fragment lengths were measured by the FiberStudio software. Genomic Vision molecular combing technology allowed hybridization of the full approximately 360-kb complement factor H gene cluster and its flanking control genes *KCNT2* and *F13B/ASPM* (total approximately 600 kb). Of the 21 samples, 19 gave satisfactory results, enabling a good overview of both alleles (except F7 and F16). Molecular combing results were determined satisfactory if the full *CFH/CFHR* gene cluster plus flanking genes were clearly visible and the gene lengths were measurable using the FiberStudio software. Hybridization signals of all patients were summarized in Supplemental Figure S1. *CFH* and each of the *CFH*-related genes of the *CFH* gene cluster were specifically labeled in a distinctive color and pattern to unequivocally differentiate between each gene (Figure 1).

Samplix Xdrop Target Enrichment and Oxford Nanopore Long-Read Sequencing

To identify the breakpoints of the *CFHR3/CFHR1* and *CFHR4/CFHR1* deletion, Xdrop indirect sequence capture (Samplix, Birkerød, Denmark) was performed in Patient F18. In short, high-molecular-weight DNA is encapsulated with a PCR mix. A short fluorescence-labeled amplicon located in close proximity to the estimated breakpoints is used to mark our region of interest. The primer pairs used to generate two different amplicons were designed to specifically bind to a region in *CFHR3* to capture the DNA fragments containing the *CFHR4/CFHR1* deletion and a region in *CFHR4* to capture the DNA fragments containing the *CFHR3/CFHR1* deletion (Figure 2). With this approach, two libraries were generated (one for each allele) per patient. Droplets containing our genomic region of interest were enriched using a FACS Aria IIIu (BD Biosciences, Franklin Lakes, NJ) by using the 100-µm nozzle at 20 psi pressure, gating based on forward scatter pulse height, side scatter pulse height, and droplet fluorescence pulse height. Droplets were sorted using the Yield precision mode for best possible recovery of

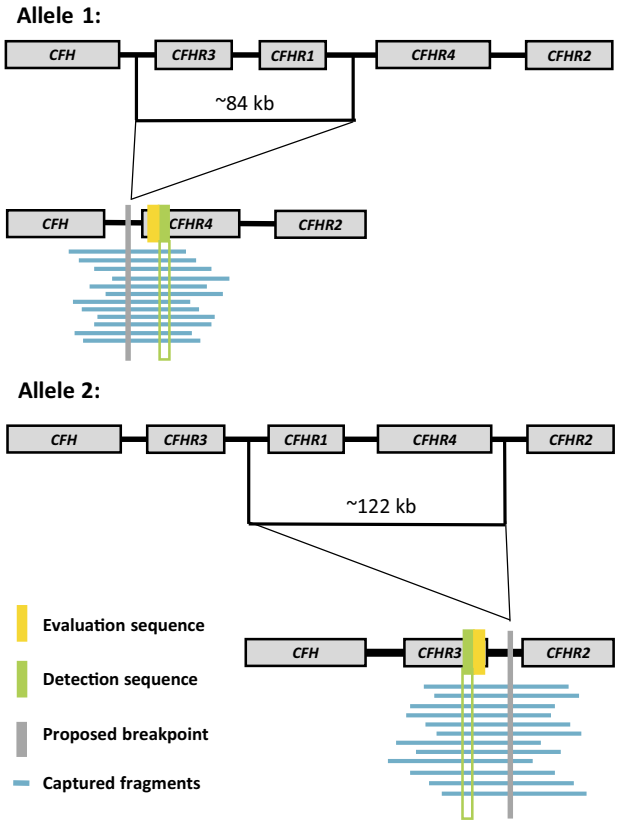

Figure 2 Schematic view of the Samplix Xdrop custom sequence capture design. (Allele 1) Detection and evaluation sequence design in *CFHR4* to identify the common *CFHR3/CFHR1* deletion. Proposed breakpoint in the intronic region between *CFH* and *CFHR3*. (Allele 2) Detection and evaluation sequence design in *CFHR3* to identify the *CFHR4/CFHR1* deletion. Proposed breakpoint in the intronic region between *CFHR3* and *CFHR2*. Primers used for the detection and evaluation sequence are listed in Table 2.

droplets of interest. The sorting of droplets is described in more detail by Madsen et al.[36] DNA is released from the isolated droplets and encapsulated again containing a multiple displacement amplification mix for target enrichment followed by long-read sequencing using a GridIon sequencing device from Oxford Nanopore (Oxford Nanopore Technologies, Oxford, UK). Sequencing reads were then aligned using the minimap2 software[37] version 2.17 (*https://github.com/lh3/minimap2*) with the prespecified *map-ont* parameter. The resulting alignment files were then sorted and indexed using samtools[38] version 1.7 (*https://github.com/samtools*) and finally visualized in the Integrative Genomics Viewer software[39] version 2.10.2 (*https://software.broadinstitute.org/software/igv*).

NGS Sequencing

For 18 patients with aHUS or C3G, custom-designed Agilent SureSelect gene panel enrichment, followed by NGS on an Illumina NextSeq500 or Illumina HiSeq 4000 platform (Illumina, San Diego, CA) of the aHUS- and C3G-associated genes *ADAMTS13*, *C3*, *CD46*, *CFB*, *CFH*, *CFHR1*, *CFHR2*, *CFHR3*, *CFHR4*, *CFHR5*, *CFI*, *DGKE*, and *MMACHC* was performed. Data were analyzed and NGS-based copy number variation (CNV) detected using the Cologne Center for Genomics Varbank2 application version 3.3 (Cologne Center for Genomics, Cologne, Germany) and the QIAGEN CLC Biomedical Genomics Workbench version 5.0.1 (Qiagen, Hilden, Germany), respectively. In particular, the approach filtered for high-quality (coverage >15-fold; phred-scaled quality >25), rare (minor allele frequency ≤0.01), and enabled CNV analysis. To exclude pipeline-related artifacts (minor allele frequency ≤0.01), the approach filtered against variants from in-house whole exome sequencing data sets. Using a comparative CNV analysis of NGS data, deviation from average coverage suggested underlying SVs in the Patients F15, F20, F18, and F3 (Figures 3A, 4A, 5A, and 6A). The annotation of *CFH* exons 1 to 23 is based on the most commonly used nomenclature to ensure compatibility.[40,41]

PCR and Sanger Sequencing

To define the breakpoints of the *CFH/CFHR1* hybrid gene, specific primers were designed that exclusively amplify a 749-bp region covering the breakpoints, as reported by Venables et al.[40] Additional primers were designed to amplify an alternative breakpoint (1017 bp) for the *CFH/CFHR1* hybrid gene found in family F15 (Table 1). Breakpoint PCR was performed for all patients, showing the *CFHR3/CFHR1* deletion in the molecular combing fluorescent *in situ* hybridization analysis because the common *CFHR3/CFHR1* deletion and the rare *CFH/CFHR1* hybrid gene could not be differentiated based on the molecular combing approach alone (data not shown). To further map the breakpoints, additional Sanger sequencing was performed for the Patients F3 and F15 (Figures 3C and 6C). Breakpoint mapping using sequencing was also performed addressing the *CFH/CFHR3* hybrid gene, the *CFHR4/CFHR1* deletion, and the common *CFHR3/CFHR1* deletion.

PCR was performed with 6 ng genomic DNA and 0.2 μmol/L of primers (Table 1) using the DNA-Taq polymerase and 10× PCR-Buffer, including 1.5 mmol/L Mg^{2+} (Analytic Jena, Jena, Germany). PCR products were visualized by gel electrophoresis using a 2% agarose gel (232-731-8; Roth, Karlsruhe, Germany) and ethidium bromide (214-984-6; Sigma-Aldrich, St. Louis, MO). PCR products were purified using the ExoSap purification kit (78200.200.UL; Thermo Fisher Scientific, Waltham, MA), according to the manufacturer's specifications. The sequence reaction was performed using the BigDye 1.1 Terminator mix (4337451; Thermo Fisher Scientific) and sequenced on the ABI Prism 3730 DNA-Analyzer platform (Applied Biosystems/Thermo Fisher Scientific).

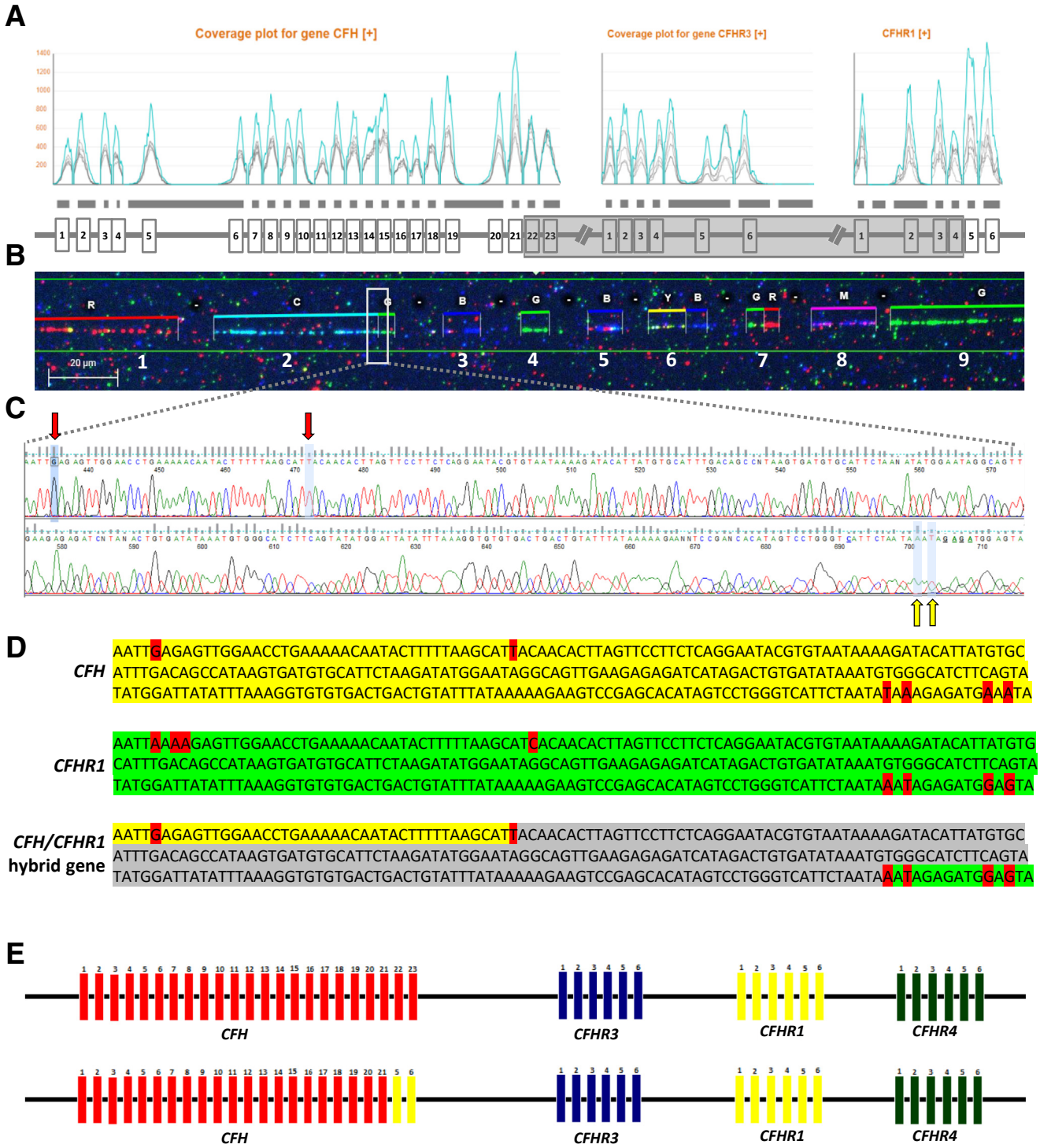

Figure 3 Patient F15. **A:** Copy number variation (CNV) visualization in Varbank2 based on CNV calling from XHMM and CONIFER. Gene coverage of single exons is shown. Patient is indicated in blue, and five controls are indicated in gray. Reduced gene coverage for exons 22 and 23 of *CFH*, normal gene coverage for *CFHR3*, and elevated gene coverage for exons 5 and 6 of *CFHR1*. **B:** Molecular combing showing the mutated allele. Wild-type allele is not shown. Fluorescent images were taken at ×40 magnification level. Validated signal with labeled genes from left ro right: red, *KCNT2* (1); cyan/green, *CFH* (2); blue, *CFHR3* (3); green, *CFHR1* (4); blue, intronic region (5); yellow/blue, *CFHR4* (6); green/red, *CFHR2* (7); magenta, *CFHR5* (8); green, *F13B* + *ASPM* (9). **C:** Breakpoint identification using PCR and Sanger sequencing (Table 1). **Red arrows** and light blue highlighted nucleotides, last nucleotides that identify the *CFH* sequence; **yellow arrows** and light blue highlighted nucleotides, first nucleotides that identify the *CFHR1* sequence. **D:** Schematic view of the breakpoint region. *CFH* sequence of the breakpoint region (yellow). *CFHR1* sequence of the breakpoint region (green). (Red) nucleotides that differ between the *CFH* and *CFHR1* sequence. Breakpoints occur within the homologous region (gray). **E:** Schematic visualization of the heterozygous *CFH/CFHR1* hybrid gene. Exons are numbered and indicated by vertical bars. *CFH* (red), *CFHR3* (blue), *CFHR1* (yellow), and *CFHR4* (green). Scale bar = 20 µm (**B**).

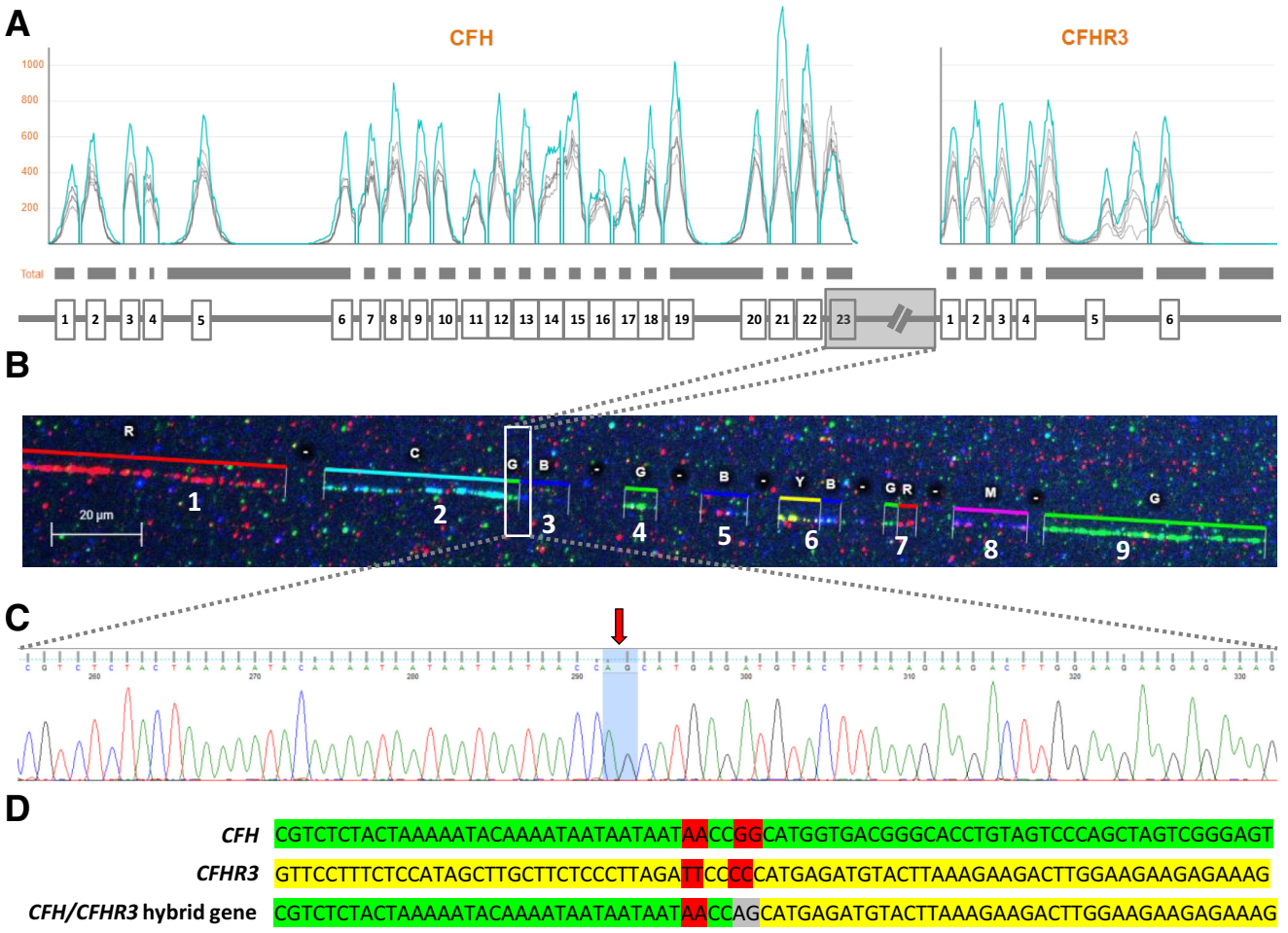

Figure 4 Patient F20. **A:** Copy number variation (CNV) visualization in Varbank2 based on CNV calling from XHMM and CONIFER. Gene coverage of single exons is shown. Patient is indicated in blue, and five controls are indicated in gray. Reduced coverage for exon 23 of *CFH*, and normal gene coverage of *CFHR3*. **B:** Molecular combing showing the *CFH/CFHR3* hybrid gene. Wild-type allele is not shown. Fluorescent images were taken at ×40 magnification level. Validated signal with labeled genes from left to right: red, *KCNT2* (1); cyan/green, *CFH* (2); blue, *CFHR3* (3); green, *CFHR1* (4); blue, intronic region (5); yellow/blue, *CFHR4* (6); green/red, *CFHR2* (7); magenta, *CFHR5* (8); green, *F13B* + *ASPM* (9). **C:** Breakpoint identification using PCR and Sanger sequencing (Table 1). **Red arrow** and light blue highlighted nucleotides, nucleotides that are different in the *CFH/CFHR3* hybrid gene sequence. **D:** Schematic view of the breakpoint region. *CFH* sequence of the breakpoint region (yellow). *CFHR3* sequence of the breakpoint region (green). (Red) nucleotides that differ between the *CFH* and *CFHR3* sequence. Sequence of the hybrid gene AG (gray) as previously described by Francis et al.[10] Scale bar = 20 µm (**B**).

Results

CFH Gene Cluster Analysis in the Screening Cohort

In total, 21 patients from 20 families were analyzed by molecular combing and sequencing (Supplemental Figure S1 and Supplemental Table S1).

The SVs previously identified in three patients (F15 and F20,[10] detailed workup shown below) with aHUS were recovered by our combined analysis approach.

In Patient F15, a *CFH/CFHR1* hybrid gene was re-identified using Sanger sequencing (Figure 3C). Primers are listed in Table 1. Patient F19 showed a *CFH/CFHR1* hybrid gene as well (data not shown), in *trans* with the common *CFHR3/CFHR1* deletion. The *CFHR3/CFHR1* deletion could be re-identified using molecular combing.

In Patient F20, molecular combing was able to visualize the previously described *CFH/CFHR3* hybrid gene that was later confirmed by Sanger sequencing (Figure 4C).

After having identified the SVs in the screening cohort, 18 additional patients with aHUS and C3G pathology were analyzed. In Patient F18, a rare *CFHR4/CFHR1* deletion was identified in *trans* with the common *CFHR3/CFHR1* deletion (Figure 5). In addition, a second rare high-penetrance *CFH/CFHR1* hybrid gene was identified in Patient F3 (Figure 6) in addition to F15. The common approximately 84-kb *CHFR3/CFHR1* deletion was found in eight patients (38.1%). Two patients were homozygous for the *CFHR3/CFHR1* deletion (F11 and F13). These two patients also showed CFH autoantibodies (DEAP-HUS). Of the 21 patients, 10 (47.6%) analyzed patients showed no structural aberrations in the *CFH* gene cluster.

Detailed Workup of Patients with Remarkable SV Findings

Patient F15: *CFH/CFHR1* Hybrid Gene

This patient presented at age 1 year and was initially treated with plasma exchange as eculizumab was not in clinical practice at that time. At age 6 years, he presented again with aHUS and was treated with eculizumab. The patient remains off dialysis 9 years later and on eculizumab treatment. Molecular combing showed no abnormalities in the structural arrangement of the *CFH* gene cluster because the C-terminal region of *CFH* and *CFHR1* both are labeled in green and *CFHR3* is still present in this variant of a *CFH/CFHR1* hybrid gene (Figure 3B). However, NGS-based CNV detection indicated the heterozygous loss of exons 22 and 23 of *CFH* and an additional copy of exons 4 and 5 of *CFHR1* (Figure 3, A and C). Presence of the *CFH/CFHR1* hybrid gene was confirmed by PCR and Sanger sequencing (Figure 3, C and D). Breakpoint PCR primers, which were used to identify the hybrid gene in Patient F3 (Table 1), failed to identify the hybrid gene variant in Patient F15, suggesting a different breakpoint in this patient. Identification of the *CFH/CFHR1* hybrid gene in Patient F15 required the design of additional primers (Table 1). The resulting heterozygous *CFH/CFHR1* hybrid gene is visualized in Figure 3E.

Patient F20: *CFH/CFHR3* Hybrid Gene

This male patient, aged 65 years, is an unaffected carrier of the mutation. He has a history of prostate cancer treated with brachytherapy in 2013, and otherwise had no other medical condition. The patient was previously described by Francis et al[10] using MLPA and Sanger sequencing approaches. The patient was included in this study to reidentify the *CFH/CFHR3* hybrid gene using the molecular combing method. NGS-based CNV detection showed the heterozygous deletion of exon 23 of *CFH* (Figure 4A). Molecular combing identified the presence of the rare heterozygous *CFH/CFHR3* hybrid gene (Figure 4B) that was confirmed by PCR and Sanger sequencing, as reported by Francis et al[10] (Figure 4, C and D).

Patient F18: Compound-Heterozygous *CFHR4/CFHR1* and *CFHR3/CFHR1* Deletion

This female patient initially developed nephrotic syndrome during pregnancy in 2013 at the age of 34 years (initial proteinuria, 8 g/day; later up to 28 g/day). The pregnancy was terminated after 22 weeks because of nephrotic syndrome and high blood pressure. A kidney biopsy was performed, which showed cellular variant focal-segmental glomerulosclerosis with a moderate degree of acute tubular lesion. The patient showed no response to immunosuppressive treatment with corticosteroids, cyclosporine, rituximab, and plasmapheresis and developed end-stage kidney disease 3 years after initial presentation; hemodialysis was started in 2016. In March 2017, the patient presented with severe neurologic symptoms (headache, nausea, and grand-mal seizures), hypertensive episode, and nephritic syndrome (vomiting, hematuria, and proteinuria). Because of an initial progression of neurologic symptoms, the patient required mechanical ventilation. Brain magnetic resonance imaging at this time showed encephalopathy with a suspicion of posterior reversible encephalopathy syndrome or acute disseminated encephalomyelitis. Cerebrospinal fluid cytology showed 88 lymphocytes/μL. Cerebrospinal fluid protein levels were elevated at 0.62 g/L (normal, <0.45 g/L), and glucose was normal. Serum creatinine was elevated at 1146 μmol/L (normal, 49 to 90 μmol/L), but serum electrolytes were within the normal range. The serologic testing for viral and bacterial causes was negative. Under a combinatorial therapy with pulsed glucocorticoids, plasmapheresis, and fresh frozen plasma infusions, the patient's neurologic symptoms improved and she could be extubated. At this time, her C3 and C4 levels were both decreased at 0.56 g/L (normal, 0.9 to 1.8 g/L) and 0.07 g/L (normal, 0.1 to 0.4 g/L), respectively. Her antinuclear antibody and antineutrophil cytoplasmic antibody titers were normal. DNA of Patient F18 was submitted for genetic testing with the clinical suspicion of a monogenic form of aHUS with central nervous system manifestations. The NGS-based CNV analysis of the *CFH* gene cluster showed evidence of a heterozygous deletion of *CFHR3* and *CFHR4* as well as the complete loss of *CFHR1* (Figure 5A). This structural aberration was confirmed by molecular combing, resolving a compound heterozygous deletion of *CFHR3/CFHR1* in *trans* with a heterozygous *CFHR4/CFHR1* deletion (Figure 5B). Breakpoint mapping was done using Oxford Nanopore long-read sequencing after long-fragment target enrichment covering the breakpoint region of the *CFHR4/1* and *CFHR3/1* deletion, respectively (Figure 5, C and D). *CFHR3/CFHR1* deletion breakpoints were refined to a 40-bp region of chromosome 1:196,733,321-196,733,362; chromosome 1:196,817,998-196,818,039 (GRCh37/hg19). *CFHR4/CFHR1* deletion breakpoints were located in a region of 385 bp between chromosome 1:196,783,258-196,783,644; chromosome 1:196,905,155-196,905,541 (GRCh37/hg19).

Patient F3: *CFH/CFHR1* Hybrid Gene

Patient F3 presented at age 16 years with diarrhea-negative hemolytic anemia and thrombocytopenia in chronic kidney disease stage 4 with focal seizures and quickly progressed to end-stage renal failure. For suspected thrombotic microangiopathy, plasma exchange was performed, but could not prevent manifestation of end-stage renal failure. Genetic testing and eculizumab were not clinical practice at that time. The patient remained on chronic hemodialysis treatment for 9 years and received a first cadaveric renal transplant at the age of 23 years. He quickly lost the renal graft 6 months later and returned to chronic hemodialysis treatment. He received a second renal graft in August 2019 under eculizumab and retained a stable graft function with creatinine levels of 120 to 130 μmol/L. A standard gene panel analysis for aHUS yielded unremarkable results, but exome-based reanalysis with bioinformatic CNV analysis

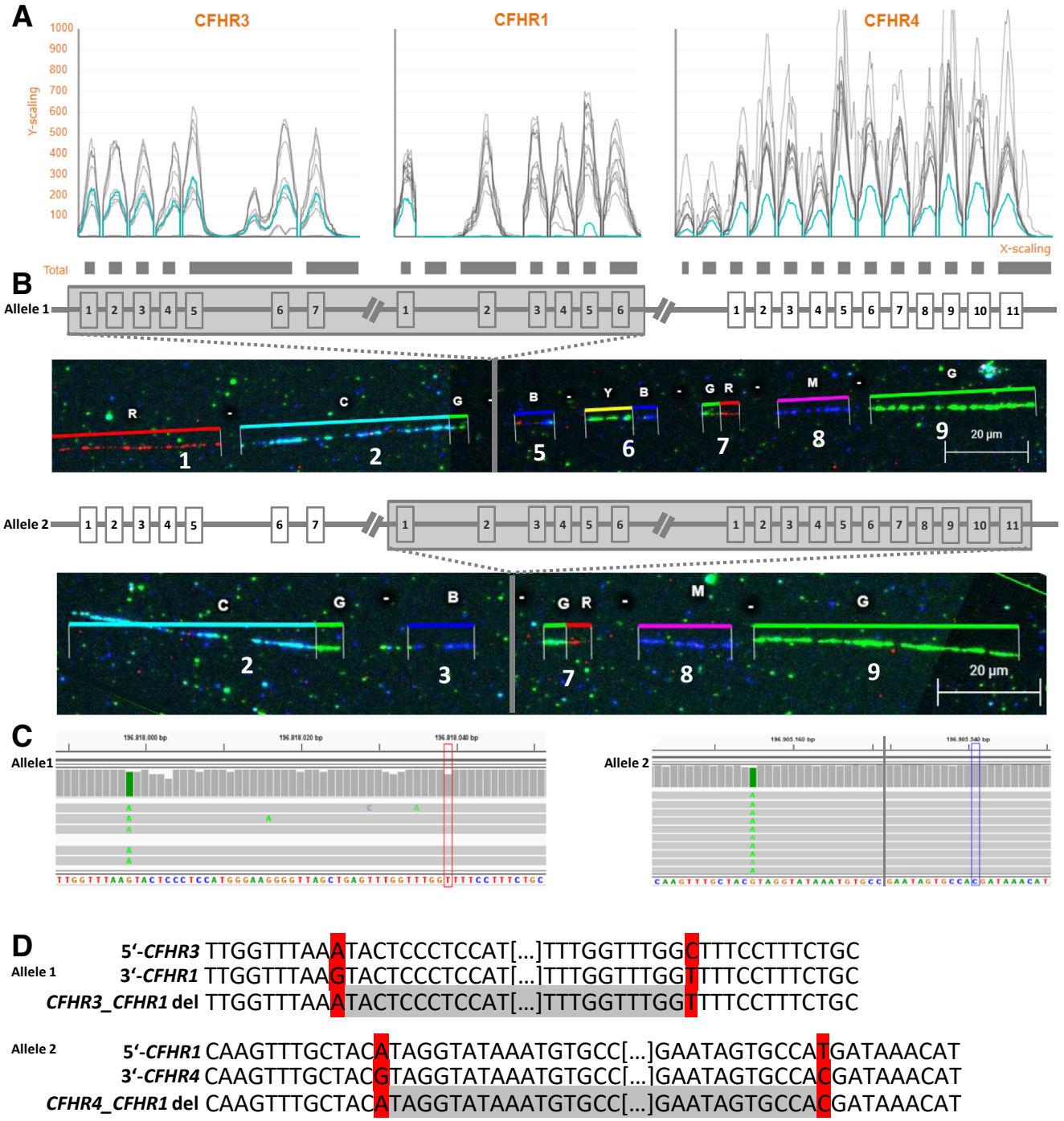

Figure 5 Patient F18. **A:** Copy number variation (CNV) visualization in Varbank2 based on CNV calling from XHMM and CONIFER. Gene coverage of single exons is shown. Patient is indicated in blue, and 10 controls are indicated in gray. (Heterozygous *CFHR3/CFHR1* deletion polymorphism in controls.) Reduced gene coverage for *CFHR3* and *CFHR4*, full loss of *CFHR1*. **B:** Molecular combing showing both alleles. Fluorescent images were taken at ×40 magnification level. Validated signal with labeled genes from left to right: red, *KCNT2* (1); cyan/green, *CFH* (2); blue, *CFHR3* (3); blue, intronic region (5); yellow/blue, *CFHR4* (6); green/red, *CFHR2* (7); magenta, *CFHR5* (8); green, *F13B* + *ASPM* (9). (Allele 1) *CFHR3/CFHR1* deletion. (Allele 2) *CFHR4/CFHR1* deletion. **C:** Breakpoint identification using Oxford Nanopore long-read sequencing after Xdrop sample preparation. (Allele 1) Nucleotide A (green) resembles the last nucleotide that identifies the 5′-*CFHR3* sequence before the breakpoint. Nucleotide T (red) resembles the first nucleotide that identifies the 3′-*CFHR1* sequence after the breakpoint. The breakpoint lies within the homologous region between the nucleotides A and T. (Allele 2) Nucleotide A (green) resembles the last nucleotide that identifies the 5′-*CFHR1* sequence before the breakpoint. Nucleotide C (blue) resembles the first nucleotide that identifies the 3′-*CFHR4* sequence after the breakpoint. The breakpoint lies within the homologous region between the nucleotides A and C. Long-read sequence of allele 2 showing the *CFHR4/CFHR1* deletion was cut to accommodate for the 385-bp homologous gap between the distinguishable nucleotide's A and C (gray vertical bar). **D:** Schematic view of the breakpoints. Single nucleotides (red) distinguish between the *CFHR4/CFHR1* and *CFHR3/CFHR1* sequences. Breakpoints occur within the homologous region of 40 bp (allele 1, *CFHR3/CFHR1* deletion) and 385 bp (allele 2, *CFHR4/CFHR1* deletion), indicated in gray. Homologous breakpoint region (gray) was shortened for visualization purposes. Scale bar = 20 µm (**B**).

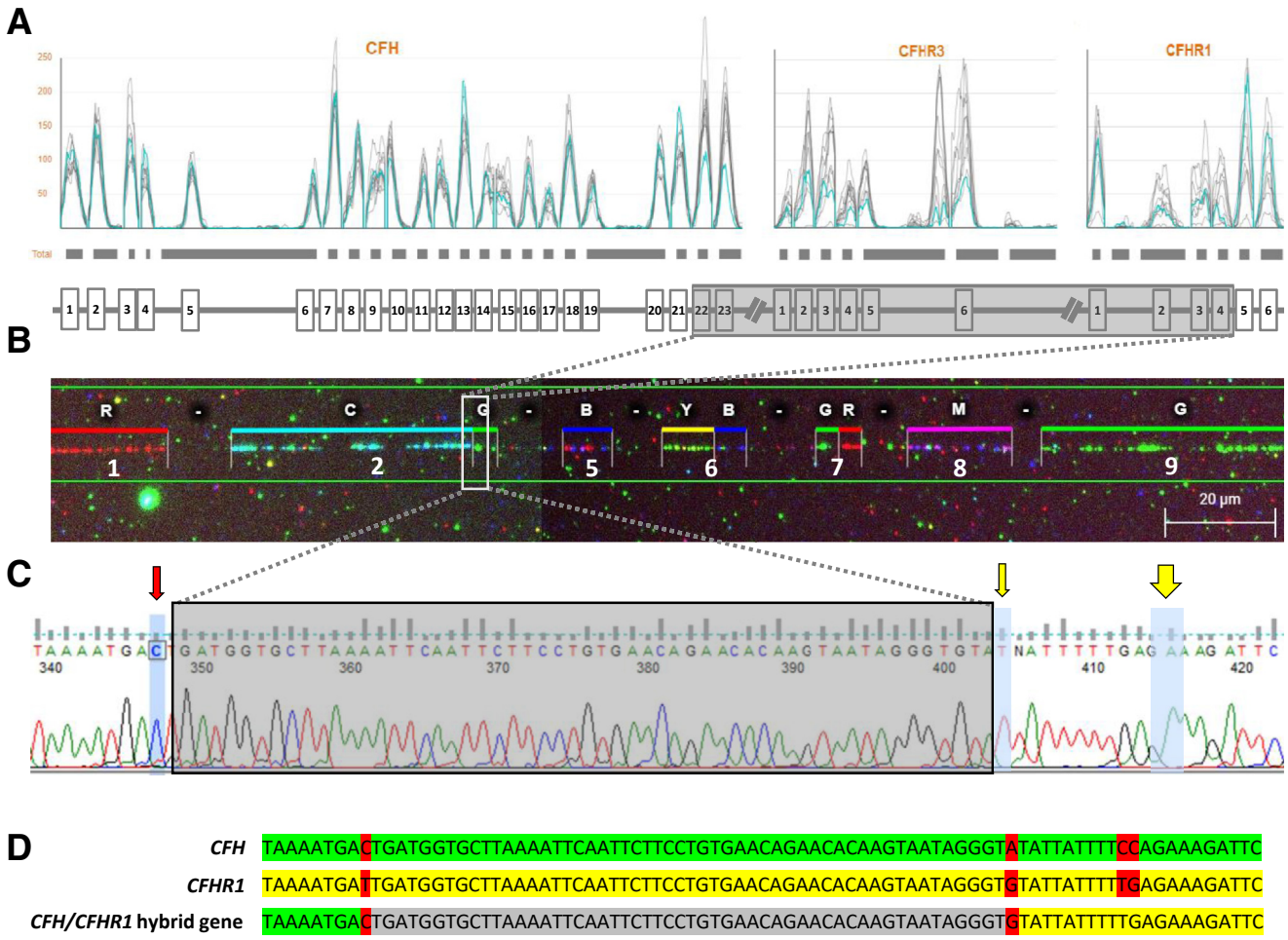

Figure 6 Patient F3. **A:** Copy number variation (CNV) visualization in Varbank2 based on CNV calling from XHMM and CONIFER. Gene coverage of single exons is shown. Patient is indicated in blue, and 10 controls are indicated in gray. Reduced gene coverage for exons 22 and 23 of *CFH*, the whole gene *CFHR3*, and exons 1 to 4 of *CFHR1*. Gene coverage of the first exon of *CFHR1* is most likely an artifact due to the high sequence homology between *CFH* and *CFHR1*. **B:** Molecular combing showing the mutated allele. Wild-type allele is not shown. Fluorescent images were taken at ×40 magnification level. Validated signal with labeled genes from left to right: red, *KCNT2* (1); cyan/green, *CFH* (2); blue, intronic region (5); yellow/blue, *CFHR4* (6); green/red, *CFHR2* (7); magenta, *CFHR5* (8); green, *F13B* + *ASPM* (9). **C:** Breakpoint identification using PCR and Sanger sequencing (primer: Table 1). **Red arrow**, last nucleotide that identifies the *CFH* sequence; **yellow arrows**, first nucleotides that identify the *CFHR1* sequence. Breakpoint region (**gray boxed area**). **D:** Schematic view of the breakpoint region. *CFH* sequence of the breakpoint region (green). *CFHR1* sequence of the breakpoint region (yellow). Breakpoints occur within the homologous region (gray). Scale bar = 20 µm (**B**).

detection indicated a heterozygous loss of exons 22 and 23 of *CFH*, of *CFHR3*, and of the first four exons of *CFHR1* (Figure 6A). Using molecular combing, the presence of a structural aberration could be confirmed in the patient, which resembled either a *CFH/CFHR1* hybrid gene or the common *CFHR3/CFHR1* deletion (Figure 6B). Breakpoint mapping using Sanger sequencing revealed the presence of the rare *CFH/CFHR1* hybrid gene and confirmed the breakpoints to be in a homologous region of 53 bp between *CFH* and *CFHR1*, identical to the hybrid gene reported by Venables et al[40] (Figure 6, C and D).

Discussion

Molecular diagnostics of patients with abnormalities in the *CFH* gene cluster can be challenging. The disease spectrum is genetically heterogeneous and characterized by a broad range of clinical manifestations, spanning from early to late onset of disease. Reduced penetrance is frequently noted in autosomal dominant forms. There are also large differences in the reported diagnostic yield, ranging from 60% to 70%[31,42,43] to in our experience much lower numbers in even purely pediatric cohorts despite comprehensive testing.

One particular disadvantage is that the routinely used methods for SV detection [ie, bioinformatic CNV detection (based on short-read NGS data) and CNV detection by MLPA] are incomplete and do not give precise structural information. Although MLPA has potential advantages compared with bioinformatic CNV analysis to uncover smaller deletions/duplications (encompassing single exons), the commercially available MLPA kit for the *CFH* gene cluster is incomplete (missing probes for all genes of the

Table 1 *CFH* Gene Cluster and Structural Aberration PCR Primer Pairs

Structural aberration	Forward primer	Reverse primer	PCR product, bp
CFH/CFHR1 hybrid gene	5′-CGGGCGGTATATTGTAACTGTTATC-3′	5′-CTGGTTTCCCTTACTCCATCTCTATT-3′	749
CFH/CFHR1 hybrid gene*	5′-CGGGCGGTATATTGTAACTGTTATC-3′	5′-CCTCTGTCATTTATTTGTTTCTGTCTG-3′	1017
CFH/CFHR3 hybrid gene	5′-CAATGGTCAGAACCACCAAAAT-3′	5′-GAAACCCACAAGGTCAGAATGAC-3′	975

*Different primer design for Patient F15.

cluster) and rearrangements without copy number changes will not be identified by either method.

For the aHUS spectrum, the exact genetic diagnosis is of utmost importance to determine the therapeutic strategy. Cost of (permanent) complement inhibition and substantial risk involved with this treatment require careful consideration of who will benefit from the expensive therapy and who will not. Genetic rearrangements in the *CFH/CFHR* gene cluster are highly correlated to post-transplant recurrence of aHUS.[8,10,40] Eculizumab, a monoclonal antibody that inhibits the cleavage of C5 into C5a and C5b and thereby blocks the formation of the membrane attack complex, has been reported to prevent the recurrence of aHUS[44,45] and has been proven beneficial in patients with aHUS caused by *CFHR3/CFHR1* deletion (DEAP-HUS),[46] *CFH/CFHR1* hybrid gene,[32] *CFHR1/CFH* hybrid gene,[7,44] and *CFH/CFHR3* hybrid gene.[9] Eculizumab as treatment in patients with the *CFHR4/CFHR1* deletion and/or *CFHR4/CFHR1* deletion in *trans* with the *CFHR3/CFHR1* deletion has not been reported yet. An overview of SVs identified in aHUS, SLE, C3G, and dense-deposit disease and available information on the use of eculizumab/complement inhibition have been summarized in Supplemental Table S2.[7,9,13–15,22,32,44,46–55]

In this study, we performed full-length structural analysis of the *CFH/CFHR* gene cluster using a multistep analysis starting with NGS, including bioinformatic CNV analysis followed by single DNA strand visualization using the molecular combing fluorescent *in situ* hybridization technique and (if applicable) finalized the in-depth screening by breakpoint identification of the *CFHR3/CFHR1* and *CFHR4/CFHR1* deletion by cost-efficient target enrichment for long read using the Xdrop targeted sequence capture instead of expensive whole-genome long-read sequencing, and succeeded in identifying new breakpoint regions, thus contributing to the growing number of deletions in the complex *CFH* gene cluster.

The most common structural aberration of the *CFH* gene cluster is the *CFHR3/CFHR1* deletion. In Patient F18, breakpoints of the common *CFHR3/CFHR1* deletion differ from the previously published breakpoints, suggesting that these vary between the individuals.[4,16,19,21] Cantsilieris et al[4] refine the breakpoints of the common *CFHR3/CFHR1* deletion to a region of 489 bp of long interspersed nuclear element repeats. The breakpoints described in this study are located approximately 6 kb upstream from the breakpoints found in our aHUS patient and approximately 10 kb upstream from the 1618-bp breakpoint region described by Hughes et al.[19] Zhao et al[16] describe the *CFHR3/CFHR1* deletion within the SLE-associated block of approximately 146 kb starting from intron 9 of *CFH* and ending downstream of *CFHR1* (chromosome 1:196,686,918-196,824,773; GRCh37/hg19) incorporating the *CFHR3/CFHR1* deletion, identified in this study as well. They presented evidence that strongly suggests the *CFHR3/CFHR1* deletion to cause an increase of SLE risk in a dosage-dependent manner by showing that homozygous individuals have a higher risk of SLE than heterozygous ones.[16]

The *CFHR4/CFHR1* deletion breakpoints (chromosome 1:196,783,258-196,905,541; GRCh37/hg19), identified in F18 and resulting in an approximately 122-kb deletion, differ from the three *CFHR4/CFHR1* deletions described by Cantsilieris et al.[4] The compound-heterozygous *CFHR3/CFHR1* and *CFHR4/CFHR1* deletion has previously been described in three patients by Moore et al,[22] who also developed factor H autoantibodies (DEAP-HUS). Antibody testing in Patient F18 yielded no pathologic findings.

Other rarely found SVs involving the CFH-related proteins have been associated with dense-deposit disease and C3G.[13,14,54] Most of these are fusion proteins that are not

Table 2 Samplx Xdrop Sequence Capture PCR Primer and Enrichment Validation qPCR Primer for the *CFHR3/CFHR1* and *CFHR4/CFHR1* Deletion

Structural aberration	Assay	Forward primer	Reverse primer
CFHR3/CFHR1 deletion	Droplet PCR	5′-ATTCTCTTGCGTCGCATCCA-3′	5′-GTCCTTCACCCGAACAGAGG-3′
	qPCR	5′-CACGGACTCCAAAAGCCACT-3′	5′-AGCTAGGAATTGTGATGCCCAA-3′
CFHR4/CFHR1 deletion	Droplet PCR	5′-ACTCCTCAAGGACTGCCAGA-3′	5′-ATCCGTGTTCTTAAAGGAAACCAC-3′
	qPCR	5′-GCTGCTTGTATTGCATTCCGT-3′	5′-GGTCTGATTCTCCTGACGCT-3′

Designed using the primer designing tool provided by Samplix (Birkerød, Denmark).
qPCR, real-time quantitative PCR.

described yet in the other pathologies, like age-related macular degeneration, SLE, or aHUS (except the *CFH/CFHR1* hybrid gene). In theory, the described SVs would have been detectable with the first-line NGS gene panel and CNV analysis and validated using the molecular combing screening approach.

In Patient F3, a *CFH/CFHR1* hybrid gene was found with the same breakpoint region to the previously reported *CFH/CFHR1* hybrid gene.[40] Maga et al[8] described a *CFH/CFHR1* hybrid gene with a different breakpoint region that resulted in an identical fusion protein. In addition, we present a third breakpoint region (in between the known breakpoint regions) resulting in yet another identical *CFH/CFHR1* fusion protein found in Patient F15. This hybrid gene is presumably generated by nonallelic or interlocus gene conversion in which exons 22 and 23 of *CFH* serve as the acceptor sequence, which is replaced by a copy of the exons 5 and 6 of *CFHR1* (donor sequence). The donor sequence, including the gene *CFHR3*, which is located between *CFH* and *CFHR1*, remains fully intact (Figure 3E). This mechanism is described in more detail by Chen et al.[56] All recombination events occur in a highly homologous region in intron 21 (ENST00000367429.9: intron 20) of *CFH* and result in the same fusion protein, suggesting a hotspot for structural recombination events. MLPA results from Patient F19 (data not shown) suggest that the breakpoints are located in intron 21 (ENST00000367429.9: intron 20) of *CFH*, similar to the other *CFH/CFHR1* hybrid genes found in this study.

Although there is no proof of clinically relevant mosaicism in aHUS at the moment, we see the technical advantage to uncover somatic structural aberrations that would remain beyond the means of detection for most currently used diagnostic methods, such as MLPA or Southern blot analysis. The principle feature of mosaicism detection has already been proven in other disease (eg, the clinical diagnostics of facio-scapulo-humeral dystrophy).[57] In addition, molecular combing allows the direct visual localization of structural variants within the gene cluster (even without loss or gain of DNA material), whereas MLPA and Southern blot analysis are limited to identify that a deletion/insertion has occurred but lacking information about the genomic localization.

This study shows that combined NGS and SV detection by molecular combing is able to enhance the detection of structural variants and can provide a more precise resolution of SVs in the genomic context, which might become important for genotype/phenotype correlations of diseases associated with the gene cluster. A cost estimation of the authors for molecular combing compared with other diagnostic methods is given in Supplemental Table S3.

Current probe design of molecular combing fails to distinguish between the frequent *CFHR3/CFHR1* deletion (which is rarely of clinical relevance) and the rare, high-penetrance *CFH/CFHR1* hybrid gene. This limitation is due to the fact that the C-terminal regions of *CFH* and *CFHR1* both are highly homologous to allow differential fluorescent labeling (Figure 1, both regions labeled in green), and can easily be resolved by a simple PCR with Sanger sequencing of the amplicon. Apart from this gap, molecular combing allows comprehensive haplotype views of the gene cluster. Visualization of single DNA molecules may help detect a wider range of structural variants for both alleles of the *CFH* gene cluster.

Acknowledgments

We thank Genomic Vision (Bagneux, France) for helping with their expertise on the custom *CFH* gene cluster probe design and molecular combing protocol. Flow cytometry experiments were performed in the FACS and Imaging Core Facility at the Max Planck Institute for Biology of Aging. Next-generation sequencing analyses were performed at the production site West German Genome Center (WGGC) Cologne.

Supplemental Data

Supplemental material for this article can be found at *http://doi.org/10.1016/j.jmoldx.2022.02.006*.

References

1. Zipfel PF, Skerka C, Hellwage J, Jokiranta ST, Meri S, Brade V, Kraiczy P, Noris M, Remuzzi G: Factor H family proteins: on complement, microbes and human diseases. Biochem Soc Trans 2002, 30(Pt 6):971−978
2. Heinen S, Sanchez-Corral P, Jackson MS, Strain L, Goodship JA, Kemp EJ, Skerka C, Jokiranta TS, Meyers K, Wagner E, Robitaille P, Esparza-Gordillo J, Rodriguez de Cordoba S, Zipfel PF, Goodship TH: De novo gene conversion in the RCA gene cluster (1q32) causes mutations in complement factor H associated with atypical hemolytic uremic syndrome. Hum Mutat 2006, 27:292−293
3. Díaz-Guillén MA, Rodríguez de Córdoba S, Heine-Suñer D: A radiation hybrid map of complement factor H and factor H-related genes. Immunogenetics 1999, 49:549−552
4. Cantsilieris S, Nelson BJ, Huddleston J, Baker C, Harshman L, Penewit K, Munson KM, Sorensen M, Welch AE, Dang V, Grassmann F, Richardson AJ, Guymer RH, Graves-Lindsay TA, Wilson RK, Weber BHF, Baird PN, Allikmets R, Eichler EE: Recurrent structural variation, clustered sites of selection, and disease risk for the complement factor H (CFH) gene family. Proc Natl Acad Sci U S A 2018, 115:E4433−E4442
5. Józsi M, Licht C, Strobel S, Zipfel SL, Richter H, Heinen S, Zipfel PF, Skerka C: Factor H autoantibodies in atypical hemolytic uremic syndrome correlate with CFHR1/CFHR3 deficiency. Blood 2008, 111:1512−1514
6. Pérez-Caballero D, González-Rubio C, Gallardo ME, Vera M, López-Trascasa M, Rodríguez de Córdoba S, Sánchez-Corral P: Clustering of missense mutations in the C-terminal region of factor H in atypical hemolytic uremic syndrome. Am J Hum Genet 2001, 68:478−484
7. Valoti E, Alberti M, Tortajada A, Garcia-Fernandez J, Gastoldi S, Besso L, Bresin E, Remuzzi G, Rodriguez de Cordoba S, Noris M: A novel atypical hemolytic uremic syndrome-associated hybrid CFHR1/CFH gene encoding a fusion protein that antagonizes factor H-dependent complement regulation. J Am Soc Nephrol 2015, 26:209−219

8. Maga TK, Meyer NC, Belsha C, Nishimura CJ, Zhang Y, Smith RJ: A novel deletion in the RCA gene cluster causes atypical hemolytic uremic syndrome. Nephrol Dial Transpl 2011, 26:739−741
9. Challis RC, Araujo GS, Wong EK, Anderson HE, Awan A, Dorman AM, Waldron M, Wilson V, Brocklebank V, Strain L, Morgan BP, Harris CL, Marchbank KJ, Goodship TH, Kavanagh D: A de novo deletion in the regulators of complement activation cluster producing a hybrid complement factor H/complement factor H-related 3 gene in atypical hemolytic uremic syndrome. J Am Soc Nephrol 2016, 27:1617−1624
10. Francis NJ, McNicholas B, Awan A, Waldron M, Reddan D, Sadlier D, Kavanagh D, Strain L, Marchbank KJ, Harris CL, Goodship TH: A novel hybrid CFH/CFHR3 gene generated by a microhomology-mediated deletion in familial atypical hemolytic uremic syndrome. Blood 2012, 119:591−601
11. Noris M, Remuzzi G: Overview of complement activation and regulation. Semin Nephrol 2013, 33:479−492
12. Zipfel PF, Wiech T, Stea ED, Skerka C: CFHR gene variations provide insights in the pathogenesis of the kidney diseases atypical hemolytic uremic syndrome and C3 glomerulopathy. J Am Soc Nephrol 2020, 31:241−256
13. Piras R, Breno M, Valoti E, Alberti M, Iatropoulos P, Mele C, Bresin E, Donadelli R, Cuccarolo P, Smith RJH, Benigni A, Remuzzi G, Noris M: CFH and CFHR copy number variations in C3 glomerulopathy and immune complex-mediated membranoproliferative glomerulonephritis. Front Genet 2021, 12:670727
14. Malik TH, Lavin PJ, Goicoechea de Jorge E, Vernon KA, Rose KL, Patel MP, de Leeuw M, Neary JJ, Conlon PJ, Winn MP, Pickering MC: A hybrid CFHR3-1 gene causes familial C3 glomerulopathy. J Am Soc Nephrol 2012, 23:1155−1160
15. Chen Q, Wiesener M, Eberhardt HU, Hartmann A, Uzonyi B, Kirschfink M, Amann K, Buettner M, Goodship T, Hugo C, Skerka C, Zipfel PF: Complement factor H-related hybrid protein deregulates complement in dense deposit disease. J Clin Invest 2014, 124:145−155
16. Zhao J, Wu H, Khosravi M, Cui H, Qian X, Kelly JA, et al: Association of genetic variants in complement factor H and factor H-related genes with systemic lupus erythematosus susceptibility. PLoS Genet 2011, 7:e1002079
17. Patel N, Adewoyin T, Chong NV: Age-related macular degeneration: a perspective on genetic studies. Eye (Lond) 2008, 22:768−776
18. Hageman GS, Hancox LS, Taiber AJ, Gehrs KM, Anderson DH, Johnson LV, Radeke MJ, Kavanagh D, Richards A, Atkinson J, Meri S, Bergeron J, Zernant J, Merriam J, Gold B, Allikmets R, Dean M; AMD Clinical Study Group: Extended haplotypes in the complement factor H (CFH) and CFH-related (CFHR) family of genes protect against age-related macular degeneration: characterization, ethnic distribution and evolutionary implications. Ann Med 2006, 38:592−604
19. Hughes AE, Orr N, Esfandiary H, Diaz-Torres M, Goodship T, Chakravarthy U: A common CFH haplotype, with deletion of CFHR1 and CFHR3, is associated with lower risk of age-related macular degeneration. Nat Genet 2006, 38:1173−1177
20. Sivakumaran TA, Igo RP Jr, Kidd JM, Itsara A, Kopplin LJ, Chen W, et al: Correction: A 32 kb critical region excluding Y402H in CFH mediates risk for age-related macular degeneration. PLoS One 2018, 13:e0209943
21. Zipfel PF, Edey M, Heinen S, Józsi M, Richter H, Misselwitz J, Hoppe B, Routledge D, Strain L, Hughes AE, Goodship JA, Licht C, Goodship TH, Skerka C: Deletion of complement factor H-related genes CFHR1 and CFHR3 is associated with atypical hemolytic uremic syndrome. PLoS Genet 2007, 3:e41
22. Moore I, Strain L, Pappworth I, Kavanagh D, Barlow PN, Herbert AP, Schmidt CQ, Staniforth SJ, Holmes LV, Ward R, Morgan L, Goodship TH, Marchbank KJ: Association of factor H autoantibodies with deletions of CFHR1, CFHR3, CFHR4, and with mutations in CFH, CFI, CD46, and C3 in patients with atypical hemolytic uremic syndrome. Blood 2010, 115: 379−387
23. Gharavi AG, Kiryluk K, Choi M, Li Y, Hou P, Xie J, et al: Genome-wide association study identifies susceptibility loci for IgA nephropathy. Nat Genet 2011, 43:321−327
24. Zhang C, Lv Q, Fan W, Tang W, Yi Z: Influence of CFH gene on symptom severity of schizophrenia. Neuropsychiatr Dis Treat 2017, 13:697−706
25. Nursal AF, Aydin PC, Pehlivan M, Sever U, Pehlivan S: UCP2 and CFH gene variants with genetic susceptibility to schizophrenia in Turkish population. Endocr Metab Immune Disord Drug Targets 2020, 21:2084−2089
26. Tang W, Liu H, Chen L, Zhao K, Zhang Y, Zheng K, Zhu C, Zheng T, Liu J, Wang D, Yu L, Fang X, Zhang C, Su KP: Inflammatory cytokines, complement factor H and anhedonia in drug-naïve major depressive disorder. Brain Behav Immun 2021, 95:238−244
27. Fakhouri F, Zuber J, Frémeaux-Bacchi V, Loirat C: Haemolytic uraemic syndrome. Lancet 2017, 390:681−696
28. Loirat C, Saland J, Bitzan M: Management of hemolytic uremic syndrome. Presse Med 2012, 41:115−135
29. Sethi S, Fervenza FC: Pathology of renal diseases associated with dysfunction of the alternative pathway of complement: C3 glomerulopathy and atypical hemolytic uremic syndrome (aHUS). Semin Thromb Hemost 2014, 40:416−421
30. Goicoechea de Jorge E, Tortajada A, García SP, Gastoldi S, Merinero HM, García-Fernández J, Arjona E, Cao M, Remuzzi G, Noris M, Rodríguez de Córdoba S: Factor H competitor generated by gene conversion events associates with atypical hemolytic uremic syndrome. J Am Soc Nephrol 2018, 29:240−249
31. Noris M, Caprioli J, Bresin E, Mossali C, Pianetti G, Gamba S, Daina E, Fenili C, Castelletti F, Sorosina A, Piras R, Donadelli R, Maranta R, van der Meer I, Conway EM, Zipfel PF, Goodship TH, Remuzzi G: Relative role of genetic complement abnormalities in sporadic and familial aHUS and their impact on clinical phenotype. Clin J Am Soc Nephrol 2010, 5:1844−1859
32. Nester C, Stewart Z, Myers D, Jetton J, Nair R, Reed A, Thomas C, Smith R, Brophy P: Pre-emptive eculizumab and plasmapheresis for renal transplant in atypical hemolytic uremic syndrome. Clin J Am Soc Nephrol 2011, 6:1488−1494
33. Hofer J, Janecke AR, Zimmerhackl LB, Riedl M, Rosales A, Giner T, Cortina G, Haindl CJ, Petzelberger B, Pawlik M, Jeller V, Vester U, Gadner B, van Husen M, Moritz ML, Würzner R, Jungraithmayr T; German-Austrian HUS Study Group: Complement factor H-related protein 1 deficiency and factor H antibodies in pediatric patients with atypical hemolytic uremic syndrome. Clin J Am Soc Nephrol 2013, 8: 407−415
34. Dragon-Durey MA, Loirat C, Cloarec S, Macher MA, Blouin J, Nivet H, Weiss L, Fridman WH, Frémeaux-Bacchi V: Anti-factor H autoantibodies associated with atypical hemolytic uremic syndrome. J Am Soc Nephrol 2005, 16:555−563
35. Hackl A, Erger F, Skerka C, Wenzel A, Tschernoster N, Ehren R, Burgmaier K, Riehmer V, Licht C, Kirschfink M, Weber LT, Altmueller J, Zipfel PF, Habbig S: Long-term data on two sisters with C3GN due to an identical, homozygous CFH mutation and autoantibodies. Clin Nephrol 2020, 94:197−206
36. Madsen EB, Höijer I, Kvist T, Ameur A, Mikkelsen MJ: Xdrop: targeted sequencing of long DNA molecules from low input samples using droplet sorting. Hum Mutat 2020, 41:1671−1679
37. Li H: Minimap2: pairwise alignment for nucleotide sequences. Bioinformatics 2018, 34:3094−3100
38. Li H, Handsaker B, Wysoker A, Fennell T, Ruan J, Homer N, Marth G, Abecasis G, Durbin R; 1000 Genome Project Data

Processing Subgroup: The sequence alignment/Map format and SAMtools. Bioinformatics 2009, 25:2078–2079
39. Robinson JT, Thorvaldsdóttir H, Winckler W, Guttman M, Lander ES, Getz G, Mesirov JP: Integrative genomics viewer. Nat Biotechnol 2011, 29:24–26
40. Venables JP, Strain L, Routledge D, Bourn D, Powell HM, Warwicker P, Diaz-Torres ML, Sampson A, Mead P, Webb M, Pirson Y, Jackson MS, Hughes A, Wood KM, Goodship JA, Goodship TH: Atypical haemolytic uraemic syndrome associated with a hybrid complement gene. PLoS Med 2006, 3:e431
41. Rodríguez de Córdoba S, Esparza-Gordillo J, Goicoechea de Jorge E, Lopez-Trascasa M, Sánchez-Corral P: The human complement factor H: functional roles, genetic variations and disease associations. Mol Immunol 2004, 41:355–367
42. Fremeaux-Bacchi V, Fakhouri F, Garnier A, Bienaimé F, Dragon-Durey MA, Ngo S, Moulin B, Servais A, Provot F, Rostaing L, Burtey S, Niaudet P, Deschênes G, Lebranchu Y, Zuber J, Loirat C: Genetics and outcome of atypical hemolytic uremic syndrome: a nationwide French series comparing children and adults. Clin J Am Soc Nephrol 2013, 8:554–562
43. Rodríguez de Córdoba S, Hidalgo MS, Pinto S, Tortajada A: Genetics of atypical hemolytic uremic syndrome (aHUS). Semin Thromb Hemost 2014, 40:422–430
44. Eyler SJ, Meyer NC, Zhang Y, Xiao X, Nester CM, Smith RJ: A novel hybrid CFHR1/CFH gene causes atypical hemolytic uremic syndrome. Pediatr Nephrol 2013, 28:2221–2225
45. Valoti E, Alberti M, Noris M: Posttransplant recurrence of atypical hemolytic uremic syndrome. J Nephrol 2012, 25:911–917
46. Zipfel PF, Mache C, Müller D, Licht C, Wigger M, Skerka C; European DEAP-HUS Study Group: DEAP-HUS: deficiency of CFHR plasma proteins and autoantibody-positive form of hemolytic uremic syndrome. Pediatr Nephrol 2010, 25:2009–2019
47. de Holanda MI, Pôrto LC, Wagner T, Christiani LF, Palma LMP: Use of eculizumab in a systemic lupus erythemathosus patient presenting thrombotic microangiopathy and heterozygous deletion in CFHR1-CFHR3: a case report and systematic review. Clin Rheumatol 2017, 36:2859–2867
48. Torres EA, Chang Y, Desai S, Chang I, Zuckerman JE, Burwick R, Kalantar-Zadeh K, Hanna RM: Complement-mediated thrombotic microangiopathy associated with lupus nephritis treated with eculizumab: a case report. Case Rep Nephrol Dial 2021, 11:95–102
49. Valoti E, Alberti M, Iatropoulos P, Piras R, Mele C, Breno M, Cremaschi A, Bresin E, Donadelli R, Alizzi S, Amoroso A, Benigni A, Remuzzi G, Noris M: Rare functional variants in complement genes and anti-FH autoantibodies-associated aHUS. Front Immunol 2019, 10:853
50. Breville G, Zamberg I, Sadallah S, Stephan C, Ponte B, Seebach JD: Case report: severe complement-mediated thrombotic microangiopathy in IgG4-related disease secondary to anti-factor H IgG4 autoantibodies. Front Immunol 2021, 11:604759
51. Togarsimalemath SK, Sethi SK, Duggal R, Le Quintrec M, Jha P, Daniel R, Gonnet F, Bansal S, Roumenina LT, Fremeaux-Bacchi V, Kher V, Dragon-Durey MA: A novel CFHR1-CFHR5 hybrid leads to a familial dominant C3 glomerulopathy. Kidney Int 2017, 92:876–887
52. Xiao X, Ghossein C, Tortajada A, Zhang Y, Meyer N, Jones M, Borsa NG, Nester CM, Thomas CP, de Córdoba SR, Smith RJ: Familial C3 glomerulonephritis caused by a novel CFHR5-CFHR2 fusion gene. Mol Immunol 2016, 77:89–96
53. Tortajada A, Yébenes H, Abarrategui-Garrido C, Anter J, García-Fernández JM, Martínez-Barricarte R, Alba-Domínguez M, Malik TH, Bedoya R, Cabrera Pérez R, López Trascasa M, Pickering MC, Harris CL, Sánchez-Corral P, Llorca O, Rodríguez de Córdoba S: C3 glomerulopathy-associated CFHR1 mutation alters FHR oligomerization and complement regulation. J Clin Invest 2013, 123:2434–2446
54. Gale DP, de Jorge EG, Cook HT, Martinez-Barricarte R, Hadjisavvas A, McLean AG, Pusey CD, Pierides A, Kyriacou K, Athanasiou Y, Voskarides K, Deltas C, Palmer A, Frémeaux-Bacchi V, de Cordoba SR, Maxwell PH, Pickering MC: Identification of a mutation in complement factor H-related protein 5 in patients of Cypriot origin with glomerulonephritis. Lancet 2010, 376:794–801
55. Medjeral-Thomas N, Malik TH, Patel MP, Toth T, Cook HT, Tomson C, Pickering MC: A novel CFHR5 fusion protein causes C3 glomerulopathy in a family without Cypriot ancestry. Kidney Int 2014, 85:933–937
56. Chen JM, Cooper DN, Chuzhanova N, Férec C, Patrinos GP: Gene conversion: mechanisms, evolution and human disease. Nat Rev Genet 2007, 8:762–775
57. Nguyen K, Walrafen P, Bernard R, Attarian S, Chaix C, Vovan C, Renard E, Dufrane N, Pouget J, Vannier A, Bensimon A, Lévy N: Molecular combing reveals allelic combinations in facioscapulohumeral dystrophy. Ann Neurol 2011, 70:627–633